

*This is the peer reviewed version of the following article: “**Dalmases, M., Linares, E., Llorca, J., Rodríguez, L. and Figuerola, A.** (2017) Exploiting metallophilicity for the assembly of inorganic nanocrystals and conjugated organic molecules. *Chemphyschem*, (17) 14: 2190–2196.” which has been published in final form at [doi: [10.1002/cphc.201600239](https://doi.org/10.1002/cphc.201600239)]. This article may be used for non-commercial purposes in accordance with [Wiley Terms and Conditions for Self-Archiving](#).”*

Exploiting Metallophilicity for the Assembly of Inorganic Nanocrystals and Conjugated Organic Molecules.

Mariona Dalmases,^{†,‡} Elisabet Aguiló,[†] Jordi Llorca,[#] Laura Rodríguez,^{†} Albert Figuerola^{*†,‡}*

*[†]Departament de Química Inorgànica, [‡]Institut de Nanociència i Nanotecnologia (IN²UB),
Universitat de Barcelona, Martí i Franquès 1-11, 08028 Barcelona, Spain; [#]Institut de
Tècniques Energètiques i Centre de Recerca en NanoEnginyeria, Universitat Politècnica de
Catalunya, Diagonal 647, 08028 Barcelona, Spain.*

KEYWORDS Au NPs, luminescent hydrogel, aurophilic interactions, hydrophilic nanocomposite, surface plasmon resonance

ABSTRACT. The accurate engineering of interfaces between plasmonic nanocrystals and semiconducting organic molecules is currently devised as a key for further developments in critical fields like photovoltaics and photocatalysis. In this work, a new and unconventional source of interface interaction based on metal-metal bonds is presented. With this aim, an Au(I)-organometallic gelator has been exploited for the formation of hydrogel-like nanocomposites containing noble metal nanoparticles and conjugated organic molecules. Noteworthy, the establishment of metallophilic interactions at the interface between the two moieties greatly

enhances the surface plasmon resonance coupling of nanoparticles in the composites. We believe that this new hybrid system might represent a promising alternative for the fabrication of improved plasmon-enhanced light harvesting devices.

INTRODUCTION

Photovoltaic devices and photocatalytic cells rely both on the possibility to harvest light and convert it into clean electrical or chemical energy.¹ In this regard, new composite photoactive materials are currently being designed to fulfill two different functions: first, performing as light antenna, so that the absorption cross-section can be enlarged and consequently more excitons (electron-hole pairs) easily generated; second, inducing an efficient charge carrier separation, so that electrons and holes can work independently in the composite material.² Plasmonic nanostructures have recently gained a lot of importance as both strong visible light absorbers and exciton dissociation enhancers in photovoltaic and photocatalytic devices.^{3,4} Indeed, in many proposed plasmon-enhanced light harvesting systems, the active material layer is formed by a blend of organic and inorganic domains, namely polymers or small conjugated organic molecules and noble metal nanoparticles (NPs) or metallic contacts, respectively.⁵⁻⁸ Thus, the study of interfaces between materials has become an issue of paramount importance in the field, and they must be accurately engineered in order to ease charge carrier percolation through the composite and consequently maximize energy conversion or photocatalytic activity.⁹⁻¹¹

An interesting approach to control the organization of organic material is the use of noncovalent, supramolecular interactions: it is well-known that semiconducting polymers and π -conjugated organic molecules can self-assemble forming functional gel-like structures based on π - π stacking that lead to superior electronic properties.^{12,13} Inorganic NPs might then be

embedded in these supramolecular systems.¹⁴ When polymeric or small organic molecule gelators are used for this purpose, the organic-inorganic interface is usually based on covalent bonds,^{15,16} electrostatic interactions,¹⁷ and/or hydrogen bonding.¹⁸

The use of metallogelators instead of only-organic gelators for the formation of either hydrogels or organogels has recently become the subject of study.^{19,20} Metallogelators are defined as low molecular weight gelators formed by the coordination of organic ligands to metallic ions. As in the case of π -conjugated organic gelators, metallogelators spontaneously self-assemble through a combination of noncovalent interactions resulting in the formation of filaments or aggregated structures. Noteworthy, the presence of a metal ion offers a new and unconventional driving force for the formation of the supramolecular structure, which lies in the possibility to establish, in some cases, metallophilic intermolecular interactions of strength comparable to the hydrogen bond.²¹ While metal-metal bonds are widely observed in solid state molecule-based crystalline systems, such source of interaction has only recently been observed in solution²²⁻²⁵ and, to the best of our knowledge, it has never been explored as a way of anchoring functional molecules to nanostructured materials in order to enhance synergetic phenomena.

We present here a new hydrosoluble nanocomposite (NCP) originated from the spontaneous supramolecular assembly of noble metal NPs and a highly fluorescent low molecular weight Au(I)-metallogelator.²⁶ These novel hybrids are characterized by intimate organometallic-inorganic interfaces that induce a strong electronic coupling between the two components, becoming in this way potential candidates for future optoelectronic devices or photocatalytic systems.

EXPERIMENTAL SECTION

The assembly of the two components leading to the formation of the hydrosoluble NCP is achieved simply by mixing two chloroform solutions at room temperature, each of them containing separately oleylamine-capped Au NPs (Au-OLAm NPs) and the luminescent gold(I) alkynyl phosphine complex [Au(4-pyridylethynyl)(DAPTA)] (Figure 1a), where DAPTA is 3,7-diacetyl-1,3,7-triaza-5-phosphabicyclo[3.3.1]nonane, hereafter called complex **1** for simplicity. Specifically, 4.2 mg (8 μ mol) of complex **1** were dissolved in 8 mL CHCl₃ and mixed with 0.17 nmol Au-OLAm NPs. The solution was shaken for 2h and centrifuged for 3 min at 4500 rpm. Then, the precipitate was washed with chloroform and the solid redispersed in polar solvents like water, methanol or ethanol forming an optically clear blue solution, as shown in Figure 1b. The formation of NCPs of complex **1** with inorganic NPs other than Au-OLAm NPs was adapted from the protocol described above using Ag/CdSe/Fe₃O₄@Au NPs instead of Au NPs. The syntheses of the inorganic NPs and complex **1** can be found in the Supporting Information (SI).

NCPs were characterized by Field Emission Scanning Electron Microscopy (FESEM) using a Zeiss Neon40 scanning electron microscope Crossbeam Station equipped with a field emission electron source operating at 5 kV. A Zetasizer NanoS Spectrometer was used for the Dynamic Light Scattering (DLS) measurements. The samples were measured in quartz cuvettes. Infrared (IR) spectra were carried out on a FTIR 520 Nicolet Spectrophotometer. For the measurements a pellet of a mixture of the sample and KBr was used. X-ray photoelectron spectroscopy (XPS) was performed on a SPECS system equipped with an Al anode XR50 source operating at 150 mW and a Phoibos 150 MCD-9 detector. The pass energy of the hemispherical analyzer was set

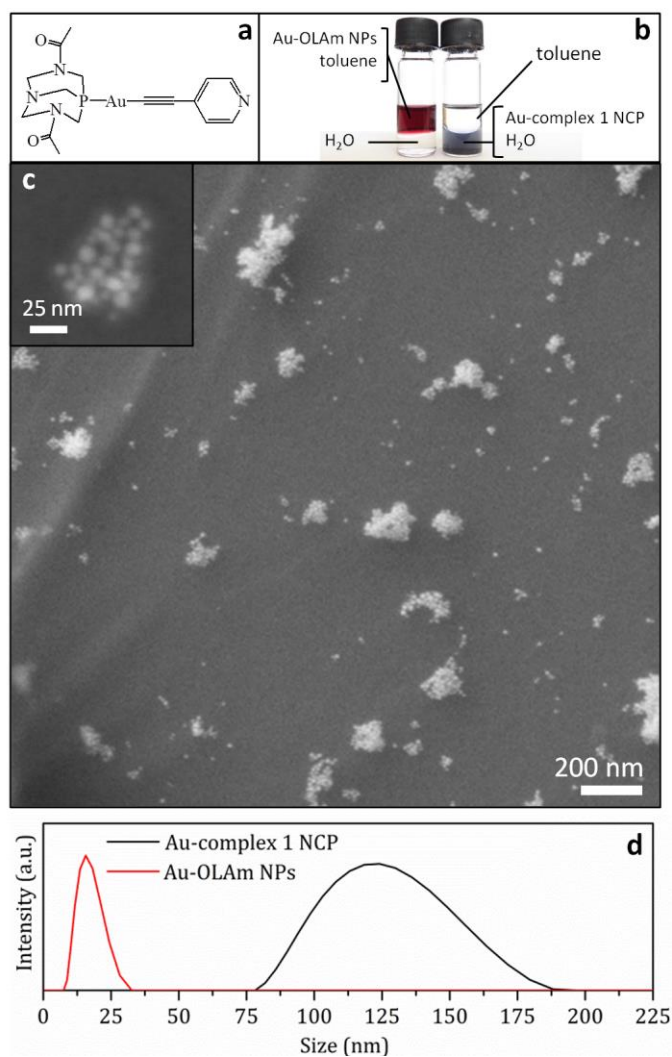
at 25 eV and the energy step was set at 0.1 eV. The binding energy (BE) values were referred to the C 1s peak at 284.8 eV. ES(+) mass spectra were recorded on a 4800Plus MALDI TOF/TOF Analyser Applied Biosystems MDS SCIEX. A Cary 100 Scan 388 Varian UV-Vis spectrophotometer and a NanoLog Horiba Jobin Yvon fluorometer were used with quartz cuvettes for optical characterization. Raman spectrum were acquired with a Jobin-YvonLabRamHR 800 spectrophotometer coupled with an Olympus BXFM optical microscope using a 532 nm laser. An Hitachi H800 MP conventional transmission electron microscope (TEM) equipped with Bioscan Gatan camera and tungsten filament, operating at an acceleration voltage of 200 kV and 3 μm spot size was used for the morphological study of all synthesized nanostructures. The samples were prepared by drop casting and evaporation of the solvent onto carbon-coated 300- μm mesh Cu grids.

The composition and concentration of the nanoparticles solutions was determined by Inductively Coupled Plasma-Atomic Emission Spectroscopy (ICP-AES). The measurements were carried out by an Optima 3200 RL Perkin Elmer spectrometer. For this measurements 50 μL of the solutions were precipitated in MeOH and re-dispersed in CHCl_3 . The solution was evaporated in an oven overnight at 90°C. 2.5 mL aqua regia and 0.7 mL H_2O_2 were added to the precipitate before the vial was sealed and then heated to 90°C for 72h. The resulting solution were transferred to 25 mL volumetric flask and diluted with milliQ water.

RESULTS AND DISCUSSION

Au-complex **1** NCP was characterized by different techniques in order to study its size and morphology. While Transmission Electron Microscopy (TEM) images confirmed that the original size and shape of the hydrophobic Au-OLAm NPs was preserved after the formation of the hydrophilic NCP (see Figure S1), Field Emission Scanning Electron Microscopy (FESEM)

showed the formation of aggregates formed by metallic particles and surrounded by a light contrasted shell of lower atomic weight, as shown in Figure 1c and inset, suggesting the presence of an organic coverage. Dynamic Light Scattering (DLS) measurements indicate that the solution is formed by colloiddally stable aggregates of average size around 117 nm as indicated in Figure 1d. The measurements revealed that the aggregates were stable in solution for long periods of



time, i.e. up to 6 months at least, at room temperature as well as at 50 °C, and at any value of pH within the range between 4 and 9 (Figures S2 and S3).

Figure 1. (a) Scheme of complex **1** molecular structure (b) Solubility of the initial hydrophobic Au-OLAm NPs and the final hydrophilic Au-complex **1** NCP (c) FESEM micrograph of Au-complex **1** NCP (d) DLS measurements of hydrophobic Au-OLAm NPs and hydrophilic Au-complex **1** NCP.

Infrared (IR) spectra of the initial hydrophobic Au NPs, free complex **1** molecules and the synthesized hydrophilic NCP sample are shown in Figure 2a. The NCP was previously washed with dichloromethane in order to discard any unbound molecules of complex **1**. The intense carboxylic C=O and pyridinic C=N stretching bands between 1500 and 1700 cm^{-1} indicate the presence of complex **1** molecules in the sample. Slight shifts to lower wavenumbers and the wider range of frequencies for the transitions observed, compared to the spectrum of free complex **1**, suggest the effective chemisorption of the molecules on the surface of the metallic nanostructures,²⁷ as well as the presence of complex **1** molecules interacting differently with NPs, forming a significantly thick envelope that confers solubility to the aggregates. Noteworthy, the intensity of the aliphatic C-H stretching bands at around 2900 cm^{-1} observed for the initial oleylamine-capped Au NPs suffers a drastic damping, evidencing the quantitative removal of the hydrophobic surfactant. Mass spectra of the sample show several characteristic peaks corresponding to the free complex **1** with additional atoms of Au, the latter being most probably knocked out from the metallic surface during the ionization process (see Figure S4). X-ray Photoelectron Spectroscopy (XPS) was also used for the chemical characterization of the NCP. XPS spectrum shown in Figure 2b proves the coexistence of Au^0 and Au(I) species in the sample, in agreement with the formation of hybrid systems containing both metallic Au NPs and an Au(I)-based metallogelator. However, the surface-sensitive character of XPS does not allow quantifying the amount of complex **1** molecules per Au NP in the sample.

Thus, this ratio has been alternatively estimated by means of UV-Vis absorption measurements, which provide a theoretical value of 2000 molecules per NP. The fitting of the XPS spectrum in the N and P regions indicates a N/P ratio of 3.6 in the NCP, in fair agreement with the theoretical ratio of 4 for complex **1**, further confirming its presence in the sample and the removal of the initial aliphatic amine surfactant (see Figure S5).

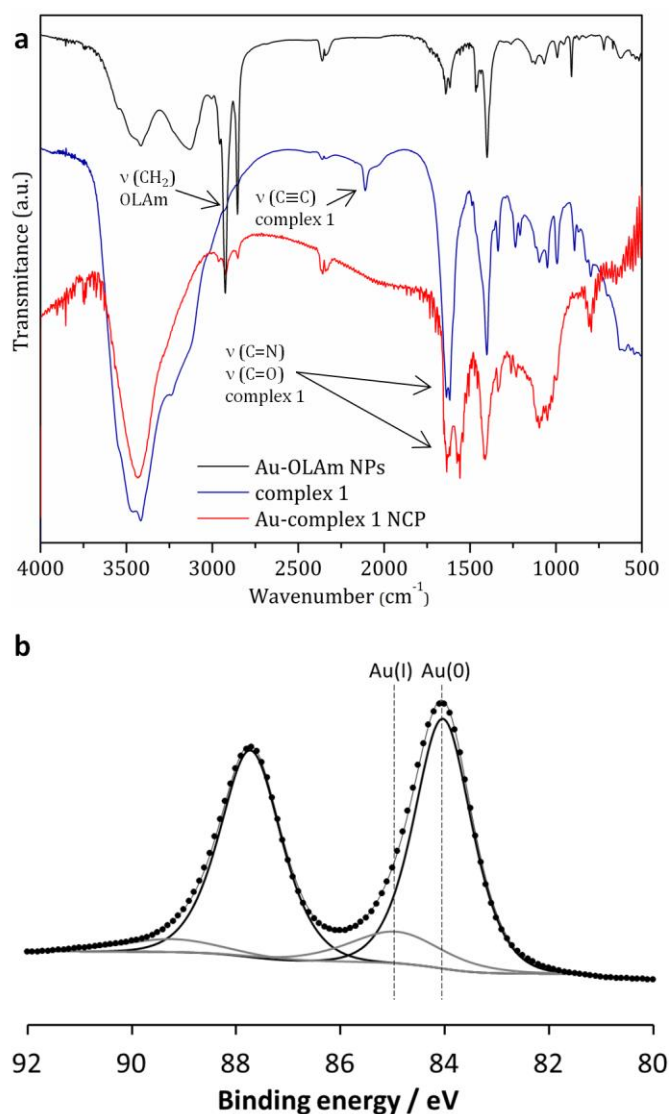


Figure 2. (a) IR spectra of Au-OLAm NPs, free complex **1**, and Au-complex **1** NCP. (b) XPS spectrum of Au-complex **1** NCP.

UV-Vis spectra of the hybrid system at different pH media present two signals as shown in Figure 3. On the one side, there is a vibronically resolved band at ~260 nm attributed to complex **1** metallochelator chromophore, which in its free form present three characteristic peaks around this wavelength.²⁶ On the other side, the signal at 500-600 nm is assigned to the characteristic surface plasmon resonance (SPR) band of gold NPs. For a better study of the NCP formation, two series of absorption spectra have been carried out fixing one of the components (complex **1** or Au-OLAm NPs) and adding small amounts of the other successively at pH 7. Both experiments (see Figure S6) show a gradual shift and widening of the SPR band. The red-shift and broadening of this band, compared to the band observed for the isolated oleylamine-capped Au NPs in toluene, denote an agglomeration of the NPs.²⁸ The collected data so far suggest that the aggregation is due to the trapping of the NPs inside the entangled complex **1**-based structures. Our previous studies showed how aqueous solutions of free complex **1** spontaneously form hydrogel structures propagated through supramolecular interactions.²⁶ Similar hydrogel structures are likely formed also in the presence of Au NPs, wrapping the latter inside and guaranteeing their water solubility. As depicted in Figure 3, the SPR band is more red-shifted and broader at neutral and slightly basic media (pH 7-8), evidencing a clear enhancement of interparticle interactions. Interestingly, in the UV-Vis spectra of water solutions of free complex **1** at pH 7-8 (see Figure S7) there is a notable intensification of the broad and weak band at 300 nm, assigned to the aurophilic interactions,²⁹ indicating a better capacity of complex **1** to create Au(I)-Au(I) bonds at this pH. Indeed, for the NCP sample, the ratio of absorption intensities at 300 nm and 260 nm (A_{300}/A_{260}) is maximum at pH 7-8, confirming the higher degree of aurophilic interactions under these specific conditions (Figure S8). Accordingly, the affinity of the metallochelator for the surface of Au NPs is greatly enhanced at neutral pH. This is translated

into a reversible change of color of the solution from violet at low (< 7) and high (> 8) pH, to blue at neutral and slightly basic medium as shown in inset of Figure 3 and in Figure S9. The enhancement of interparticle SPR coupling originating the red shift and broadening of the SPR band at pH 7-8 can be mainly associated to an increase of aurophilic interactions in the NCP, since no significant shrinkage or variation of size of the aggregates is observed by DLS measurements in samples at different pH (Figure S3).^{17,30} Although these results confirm the key role of metallophilic bonds in the system, the interaction of the surface atoms of Au NPs with complex **1** through the pyridinic nitrogen atom of the latter should not be neglected: the successful transfer of metallic nanostructures from organic solvents to water solutions by means of only-organic pyridine derivatives has been previously reported by other authors.^{31,32}

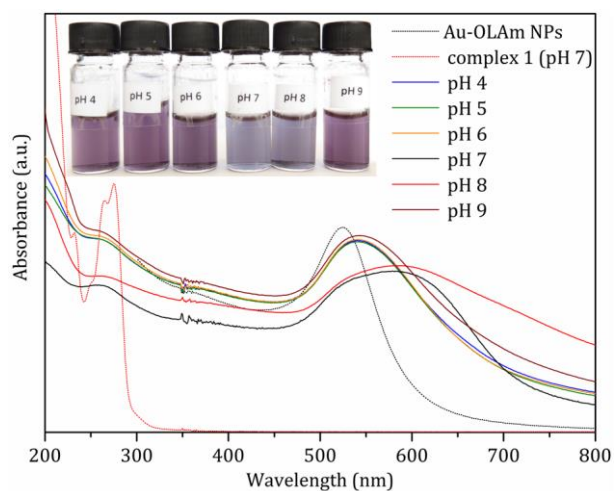


Figure 3. UV-Vis absorption spectra of hydrophilic Au-complex **1** NCP at different pH media, hydrophobic Au-OLAm NPs in toluene and free complex **1** at neutral pH. For ease of understanding, the spectrum of Au-OLAm NPs in toluene is shown only above 300 nm, avoiding the appearance of solvent absorption in the figure. (inset) Au-complex **1** NCP water dispersions at different pH media.

The efficient quantitative quenching of fluorescence of complex **1** observed in the Au-complex **1** NCP,^{33,34} and the surface enhanced Raman scattering processes (SERS) experienced by complex **1** molecules bound onto and placed in the proximity of plasmonic NPs,³⁵ allowed studying our system by Raman spectroscopy as shown in Figure S10. Strong bands are observed at ca. 1650-1500 cm^{-1} , that can be assigned to the carbonyl and C=N vibrations of the organometallic complex. Remarkably, the Raman spectrum allows also confirming the presence of the C \equiv C bond of complex **1**, characterized by a broad band at 2050 cm^{-1} , which could not be observed in the NCP sample by infrared spectroscopy.

All in all, these data confirm the formation of hydrosoluble Au-complex **1** NCPs and illustrate how aurophilic interactions strengthen the interface between the inorganic NPs and the organometallic gelator, and enhance the interparticle SPR coupling. In order to further confirm these evidences, additional experiments were made replacing Au NPs by other types of inorganic nanocrystals of similar sizes but different chemical nature. Ag NPs as well as CdSe quantum dots and Fe₃O₄ nanocrystals were chosen as representative systems. Ag NPs behave in an analogous way to that of Au NPs (see Figures S11-S15). Metallophilic Ag-Au interactions are expected to play an important role in this system as well as they do in many supramolecular assemblies of organometallic molecules.³⁶ On the contrary, no hydrophilic materials were obtained when replacing Au NPs by CdSe or Fe₃O₄ nanocrystals. This behavior is believed to be due to the absolute lack of affinity between the surface of these inorganic NPs and complex **1**, most probably related to their inability to form metallophilic interactions. However, a fine atomic Au coating of the surface of Fe₃O₄ nanocrystals was sufficient so as to improve their affinity for complex **1** and obtain stable aqueous solutions of Fe₃O₄@Au-complex **1** NCPs (see Figure S16).

CONCLUSIONS

A new strategy is presented for the functionalization and coupling of noble metal plasmonic NPs with conjugated organic moieties by means of direct metal-metal bonds. With this purpose, a small molecule conjugated metallogelator has been used, which is characterized by the presence of a Au(I) ion covalently linked to a short conjugated π system, with the ability to establish strong metallophilic interactions with the surface atoms of Au and Ag NPs. Such new source of chemical affinity induces the room temperature formation of stable NCPs that are soluble in water and alcohol solutions. We believe that this type of system could represent a significant improvement in terms of interface design between plasmonically active NPs and photoactive polymers, since metallogelators are prone to create a direct link between surface atoms of metallic nanostructures and π - π stacking systems in semiconducting polymers, chemically smoothing their interface. Thus, significant improvements in the field of plasmon enhanced light harvesting devices are expected thereof. The potential of other organometallic gelators for the successful functionalization of inorganic NPs, as well as the capacity of these novel NCPs to form functional blends of materials, are currently being addressed.

ASSOCIATED CONTENT

Supporting Information.

Experimental details; TEM, DLS, mass spectrometry, XPS and UV-Visible characterization of free complex **1**, Au-OLAm NPs and/or Au-complex **1** NCPs; morphological and chemical characterization of Ag-complex **1** NCPs; morphological characterization of Fe₃O₄@Au-complex **1** NCPs.

AUTHOR INFORMATION

Corresponding Author

* albert.figueroa@qi.ub.es, laura.rodriguez@qi.ub.es

Notes

The authors declare no competing financial interests.

ACKNOWLEDGMENT

We acknowledge financial support from the Spanish MINECO through CTQ2012-32247 and CTQ2012-31335 and from the Generalitat de Catalunya through 2014 SGR 129. A. F. acknowledges the Spanish MINECO for a Ramón y Cajal Fellowship (RYC-2010-05821). J.L. is Serra Húnter Fellow and is grateful to ICREA Academia program.

REFERENCES

- (1) Likhtenshtein, G. I. *Solar Energy Conversion: Chemical Aspects*; John Wiley & Sons, Inc., 2012.
- (2) Su, Y. W.; Lin, W. H.; Hsu, Y. J.; Wei, K. H. *Small* **2014**, *10* (22), 4427-4442.
- (3) Atwater, H. A.; Polman, A. *Nat. Mater.* **2010**, *9* (3), 205-213.
- (4) Wang, C.; Astruc, D. *Chem. Soc. Rev.* **2014**, *43*, 7188-7216.
- (5) Kang, M. G.; Xu, T.; Park, H. J.; Luo, X.; Guo, L. J. *Adv. Mater.* **2010**, *22* (39), 4378-4383.
- (6) Lu, L.; Luo, Z.; Xu, T.; Yu, L. *Nano Lett.* **2013**, *13* (1), 59-64.

- (7) Jägeler-Hoheisel, T.; Selzer, F.; Riede, M.; Leo, K. *J. Phys. Chem. C* **2014**, *118* (28), 15128-15135.
- (8) Park, H. Il; Lee, S.; Lee, J. M.; Nam, S. A.; Jeon, T.; Han, S. W.; Kim, S. O. *ACS Nano* **2014**, *8* (10), 10305-10312.
- (9) Kamat, P. V. *Acc. Chem. Res.* **2012**, *45* (11), 1906-1915.
- (10) Bansal, N.; Reynolds, L. X.; MacLachlan, A.; Lutz, T.; Ashraf, R. S.; Zhang, W.; Nielsen, C. B.; McCulloch, I.; Rebois, D. G.; Kirchartz, T.; Hill, M. S.; Molloy, K. C.; Nelson, J.; Haque, S. A. *Sci. Rep.* **2013**, *3*, 1531.
- (11) Ben-Shahar, Y.; Scotognella, F.; Waiskopf, N.; Kriegel, I.; Dal Conte, S.; Cerullo, G.; Banin, U. *Small* **2015**, *11* (4), 462-471.
- (12) Praveen, V. K.; Ranjith, C.; Bandini, E.; Ajayaghosh, A.; Armaroli, N. *Chem. Soc. Rev.* **2014**, *43*, 4222-4242.
- (13) Park, Y. D.; Lee, S. G.; Lee, H. S.; Kwak, D.; Lee, D. H.; Cho, K. *J. Mater. Chem.* **2011**, *21* (7), 2338-2343.
- (14) Kao, J.; Thorkelsson, K.; Bai, P.; Rancatore, B. J.; Xu, T. *Chem. Soc. Rev.* **2013**, *42* (7), 2654-2678.
- (15) Ren, S.; Chang, L.-Y.; Lim, S.-K.; Zhao, J.; Smith, M.; Zhao, N.; Bulović, V.; Bawendi, M.; Gradecak, S. *Nano Lett.* **2011**, *11* (9), 3998-4002.
- (16) Albero, J.; Riente, P.; Clifford, J. N.; Pericàs, M. A.; Palomares, E. J. *J. Phys. Chem. C* **2013**, *117*, 13374-13381.

- (17) Lim, S.; Song, J. E.; La, J. A.; Cho, E. C. *Chem. Mater.* **2014**, *26* (10), 3272-3279.
- (18) Jang, S. G.; Kramer, E. J.; Hawker, C. J. *J. Am. Chem. Soc.* **2011**, *133* (42), 16986-16996.
- (19) Zhang, J.; Su, C. Y. *Coord. Chem. Rev.* **2013**, *257* (7-8), 1373-1408.
- (20) Lima, J. C.; Rodríguez, L. *Inorganics* **2015**, *3* (1), 1-18.
- (21) Schmidbaur, H.; Schier, A. *Chem. Soc. Rev.* **2012**, *41* (1), 370-412.
- (22) Kishimura, A.; Yamashita, T.; Aida, T. *J. Am. Chem. Soc.* **2005**, *127* (1), 179-183.
- (23) Strassert, C. A.; Chien, C. H.; Galvez Lopez, M. D.; Kourkoulos, D.; Hertel, D.; Meerholz, K.; De Cola, L. *Angew. Chemie - Int. Ed.* **2011**, *50* (4), 946-950.
- (24) Gavara, R.; Llorca, J.; Lima, J. C.; Rodríguez, L. *Chem. Commun.* **2013**, *49*, 72-74.
- (25) Gavara, R.; Aguiló, E.; Fonseca Guerra, C.; Rodríguez, L.; Lima, J. C. *Inorg. Chem.* **2015**, *54*, 5195-5203.
- (26) Aguiló, E.; Gavara, R.; Lima, J. C.; Llorca, J.; Rodríguez, L. *J. Mater. Chem. C* **2013**, *1* (35), 5538-5547.
- (27) Xian, J.; Hua, Q.; Jiang, Z.; Ma, Y.; Huang, W. *Langmuir* **2012**, *28* (17), 6736-6741.
- (28) Ghosh, S. K.; Pal, T. *Chem. Rev.* **2007**, *107* (11), 4797-4862.
- (29) Rodríguez, L.; Ferrer, M.; Crehuet, R.; Anglada, J.; Lima, J. C. *Inorg. Chem.* **2012**, *51* (14), 7636-7641.
- (30) Srivastava, S.; Frankamp, B. L.; Rotello, V. M. *Chem. Mater.* **2005**, *17* (3), 487-490.

(31) Gittins, D. I.; Caruso, F. *Angew. Chemie - Int. Ed.* **2001**, *40* (16), 3001-3004.

(32) Gandubert, V. J.; Lennox, R. B. *Langmuir* **2005**, *21* (14), 6532-6539.

(33) Kühn, S.; Håkanson, U.; Rogobete, L.; Sandoghdar, V. *Phys. Rev. Lett.* **2006**, *97* (1), 017402.

(34) Rosa, J. P.; Lima, J. C.; Baptista, P. V. *Nanotechnology* **2011**, *22*, 415202.

(35) Schlücker, S. *Angew. Chemie - Int. Ed.* **2014**, *53* (19), 4756-4795.

(36) Fernandez, E. J.; Lopez-de-Luzuriaga, J. M.; Monge, M.; Rodriguez, M. A.; Crespo, O.; Gimeno, M. C.; Laguna, A.; Jones, P. G. *Chem. - A Eur. J.* **2000**, *6* (4), 636-644.

